Optimum Antireflection Coatings for Heteroface AlGaAs/GaAs Solar Cells—Part II: The Influence of Uncertainties in the Parameters of Window and Antireflection Coatings

IGNACIO REY-STOLLE[1,2] and CARLOS ALGORA[1]

1.—Instituto de Energía Solar (UPM), ETSI de Telecomunicación, Avda. Complutense s/n, 28040 Madrid, Spain. 2.—e-mail: irey@ies-def.upm.es

This paper details both theoretical and experimental results of an enhanced model to design MgF_2/ZnS double-layer antireflection coatings for AlGaAs/GaAs heteroface solar cells. The main contribution of this work is that a method for taking technological tolerances or uncertainties into account in the optically relevant parameters for antireflection coating design is presented. This is done by the calculation of contours of quasi-optimum performance for a certain range of variation of the uncertain parameters. A number of experiments testing different aspects of the predictions made by the model are commented on, showing good agreement with the calculated performance. Unwanted window oxidation, described in Part I of this work, has proven to be the key factor influencing quasi-optimum contours.

Key words: AlGaAs/GaAs solar cells, antireflection coatings, high efficiency

INTRODUCTION

Nowadays, the application of antireflection coatings (ARC) is an essential and widespread process in the manufacturing of high efficiency AlGaAs/GaAs solar cells both in industry and research. An introduction to the philosophy and problems surrounding ARC design can be found in Part I[1] of this paper as well as in the abundant literature on the subject.[2–6] In Part I of this work the influence of unwanted oxidation of the AlGaAs window layer was studied both theoretically and experimentally and was proven to have a key influence on ARC design. In this work it was also suggested that uncertainty in important optical parameters could also be responsible for the frequent misfit between theory predictions and values for short circuit current (J_{SC}) actually achieved after ARC deposition. Obviously, the sound knowledge of ARC design together with the small but frequent mismatch between theory and practice are difficult facts to marry. Either the model is incomplete and thus cannot describe some aspects of the physical reality (which happened in Part I with the oxide layer) or it is being fed with the wrong input parameters. The latter hypothesis is explored in this paper.

As a matter of fact, in the referenced literature on ARC design for AlGaAs/GaAs heteroface solar cells[2–6] there seems to be a very accurate knowledge of all the parameters of optical relevance. Conversely, in actual production conditions there is not. For instance, the exact content of aluminum (x_{Al}) and/or the thickness of the window layer (W_{IW}) might be only approximate. In addition, the oxide layer on top of the window of significant optical relevance[1] might be totally unknown. Moreover, the technological process for ARC deposition could augment the uncertainty level by adding some error in ARC layer thickness, by imposing some dispersion in thickness distribution or in general by perturbing the homogeneity or accuracy of optically meaningful properties of the coatings.

It is clear that there is an accurate theoretical model for ARC design on AlGaAs/GaAs solar cells but it is also evident that in some cases it might be fed with uncertain parameters yielding some discrepancy between theory and empirical results. Accordingly, the aim of the present paper is to include uncertainty analysis into the well-stated theory for optimum ARC calculation. To achieve this goal the theoretical basis summarized in Ref. 2 is enriched with a model for the parasitic oxidation of the window layer of Ref. 1 and then a sensitivity analysis of optimum ARC design versus its main parameters is carried out. The basis of this analysis is the calculation of the quasi-optimum performance contours,[7,8]

(Received January 5, 2000; accepted March 6, 2000)

i.e., areas that define optimum ARCs for a range of possible window parameters. The MgF_2/ZnS—acting as a double-layer antireflection coating (DARC)—is the only combination of materials used in the calculations as it is widely considered to be the optimum choice[1–6] and illustrates a case of sufficient complexity (two ARC layers). Consequently, a comprehensive and realistic model for ARC design is set up. Finally, the proposed model is tested experimentally, validated and then some practical conclusions and suggestions are summarized.

MODEL: THE QUASI-OPTIMUM DARC REGIONS

As previously mentioned, the philosophy and model for the calculations in this paper are the same as those in Part I.[1] Consequently, the structure used for optical calculations can be found in Fig. 1 in Part I.[1] The fixed and optimized parameters as well as the optical constants are summarized in Table I in Part I.[1] The calculation and optimization procedure is also described in that same reference.

The optimum DARC for different configurations will be the starting point for the contour calculation but before doing that let us examine the evolution of the short circuit current in the surroundings of that optimum DARC to gain more insight to the problem of sensitivity. Figure 1 shows the variation of short circuit current versus the thickness of the top MgF_2 layer (W_{MgF2}) and the bottom ZnS layer thickness (W_{ZnS}) for the non-oxidation case and an arbitrarily chosen $Al_{0.85}Ga_{0.15}As$-window thickness of 30 nm. In each curve the counterpart layer thickness (ZnS thickness for MgF_2 layer and vice versa) is kept constant and equal to the optimum value. A first remarkable consequence of both plots is the low slope (notice that the y-axis is highly zoomed) of the curve near its maximum (interval painted with a thick solid line). This means that covering the cell with a DARC including a MgF_2 layer slightly shifted from the optimum position would cause a minimal loss in short circuit current for that particular set of parameters. Therefore we could say that there is an interval (of around 30 nm wide as shown in Fig. 1) of quasi-optimum W_{MgF2} values, any of them virtually leading to the maximum short circuit current. The ZnS layer shows this same general behavior but with a shorter length for such a quasi-optimum interval (Fig. 1 shows some 18 nm).

Probably, when shifting simultaneously both MgF_2 and ZnS layer thickness from their optima values, a set of quasi-optimum DARCs with a negligible difference in performance with the optimum case can be also found. This set of DARCs can be represented as an area in the bidimensional space formed by W_{ZnS} (x-axis) and W_{MgF2} (y-axis) as shown in Fig. 2 (which will be described later on). In our work, the strategy followed for the calculation of the quasi-optimum DARC areas was to recalculate the short circuit current in the surroundings of the optimum value until a drop higher than that established as the limit value

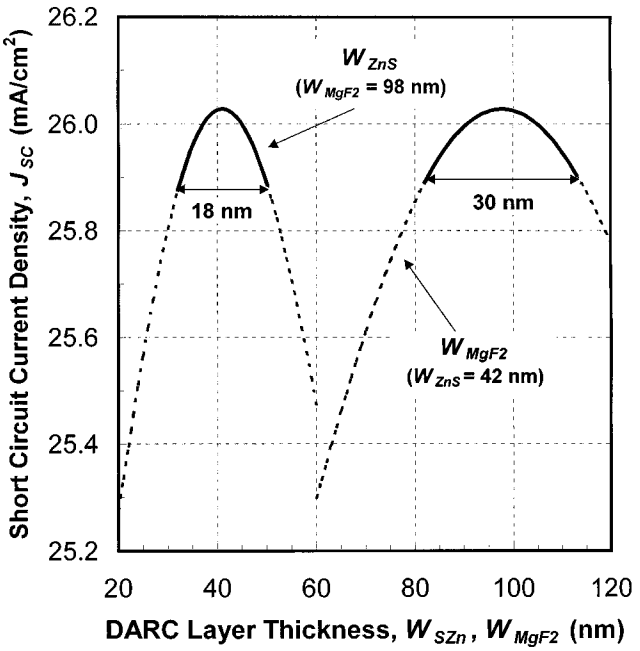

Fig. 1. The evolution of the short circuit density (J_{SC}) with (a) ZnS layer thickness and (b) MgF_2 layer thickness for a $Al_{0.85}Ga_{0.15}As$-window 30 nm thick. In each curve the counterpart layer thickness (ZnS thickness for MgF_2 layer and vice versa) is kept constant and equal to the optimum for each oxide.

Table I. The Calculated Optimum MgF_2/ZnS DARC for Non-oxidized Windows

W_{IW} (nm)	W_{ZnS} (nm)	W_{MgF2} (nm)
20	40	95
30	41	98
40	44	101
50	47	104

was found. The maximum short circuit current drop was arbitrarily set to 0.2 mA/cm^2 (it represents around 1% of the typical value for J_{SC} for our uncoated AlGaAs/GaAs solar cells). This process leads to the finding of a contour around the optimum DARC value containing a quasi-optimum DARC region. Similar approaches can be found in Refs. 7 and 8.

In the following subsections we will firstly apply the calculation of quasi-optimum DARC regions to the study of the non-oxidized AlGaAs window (classical case) to bind the incidence of window thickness (W_{IW}) and aluminum content (x_{Al}) in DARC design. Afterwards the case of an oxidized AlGaAs window will be thoroughly analyzed.

Quasi-optimum DARC Design for Non-oxidized AlGaAs Windows

In Fig. 2 quasi-optimum DARC areas for $x_{Al} = 0.7, 0.8$, and 0.9 and $W_{IW} = 20$, 30, 40, and 50 nm are depicted. As seen in Fig. 2 no significant difference exists between the aluminum contents considered. In that plot thick solid lines ($x_{Al} = 0.7$), thin solid lines ($x_{Al} = 0.8$) and dashed lines ($x_{Al} = 0.9$) practically overlap for

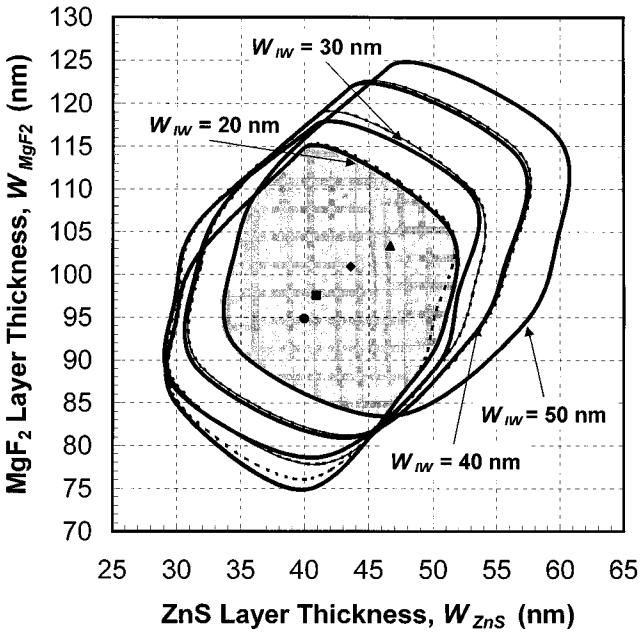

Fig. 2. The quasi-optimum DARC areas for x_{Al} = 0.7 (thick solid lines), x_{Al} = 0.8 (thin solid lines) and x_{Al} = 0.9 (dashed lines) each one plotted for W_{IW} = 20 nm to 50 nm as quoted. Optimum DARCs are also printed: W_{IW} = 20 nm (●), W_{IW} = 30 nm (■), W_{IW} = 40 nm (◆) and W_{IW} = 50 nm (▲).

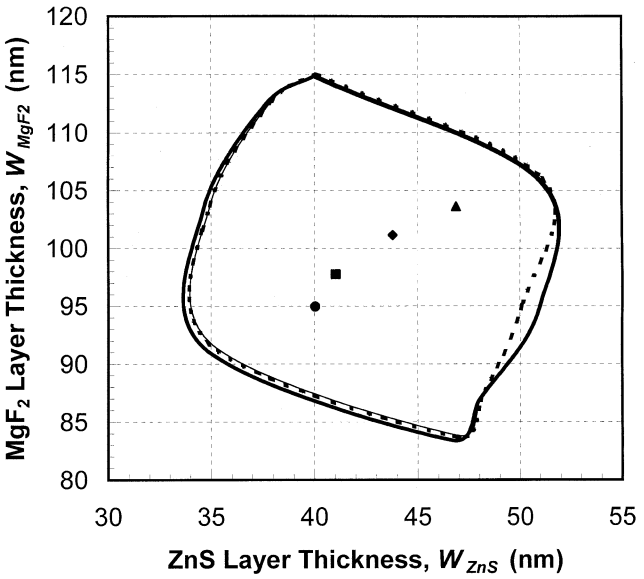

Fig. 3. The quasi-optimum DARC areas for any window layer thickness between 20 nm and 50 nm (resulting from the intersection of all quasi-optimum DARC areas for each window thickness). Thick solid lines are used for x_{Al} = 0.7, thin solid lines for x_{Al} = 0.8 and dashed lines for x_{Al} = 0.9. Optimum DARCs are also printed: W_{IW} = 20 nm (●), W_{IW} = 30 nm (■), W_{IW} = 40 nm (◆) and W_{IW} = 50 nm (▲).

every window thickness considered. Hence the quasi-optimum DARC region (i.e., DARC design) seems to be virtually insensitive to variations of the aluminum content of the window in the range useful for solar cell application (i.e., high bandgap, thus high x_{Al}). On the other hand, window layer thickness has a greater incidence in quasi-optimum DARC regions. Thick window layers tend to have larger quasi-optimum areas—more or less with the same shape—with the center (optimum DARC) located in both high MgF_2 and ZnS thickness values. Conversely thin window layers tend to have smaller quasi-optimum DARC areas (but still big) with the center displaced to lower values for both MgF_2 and ZnS layer thickness.

Let us consider the center of Fig. 2 (shadowed) which is also magnified in Fig. 3. This is an area defined by the intersection of all quasi-optimum areas each of which are calculated for a certain window thickness (remember that the influence of x_{Al} is negligible). This area represents a quasi-optimum DARC region for all window thicknesses (from 20 nm to 50 nm) and for all aluminum contents (from 0.7 to 0.9). Thus any DARC made up of a couple of W_{MgF2} and W_{ZnS} values belonging to this region will guarantee almost maximum short circuit current provided that the actual window parameters are within the aforementioned intervals. In fact all optimum DARCs for the individual cases (summarized in Table I) lie within this area which is indeed rather large.

This result is in complete agreement with the common belief that optimum DARCs do not really require much effort either theoretically or technologically since a rough approximation to the optimum will provide outstanding results. However, our approach has added quantitative limits for such a rough approximation by defining the quasi-optimum DARC for a wide range of windows. Another consequence of this result is that uncertainties in initial window parameters cannot be the cause of losses in short circuit current when, after DARC deposition, lower values than those expected are actually achieved. Other issues with a greater incidence in DARC design—such as AlGaAs window layer oxidation as suggested—must have a key role in dropping short circuit current.

Quasi-optimum DARC Design for Oxidized AlGaAs Windows

The quasi-optimum DARC regions calculated for several oxidation stages and window layer thickness can be seen in Fig. 4a to d. In these calculations the aluminum composition has been kept constant and equal to x_{Al} = 0.85 since—as has been shown in the previous section—the incidence of aluminum content is negligible.

This time, for reasons of clarity, there is a separate figure for each window layer thickness with four quasi-optimum DARC regions plotted. Each one of those regions takes a certain oxidation stage into account, namely no oxide, slight oxidation (W_{Ox} =8 nm), medium oxidation (W_{Ox} =16 nm) and heavy oxidation (W_{Ox} =24 nm). As these regions overlap we are sure that all intermediate cases are considered. Of course the non-oxidation case is exactly the one analyzed in the previous section. However there are some new oxide-induced interesting features. When an oxide layer grows there is a displacement of the quasi-optimum DARC area center (i.e., optimum DARC) to lower values of both W_{MgF2} and W_{ZnS}. Such a displacement is mainly related to the similar optical role that

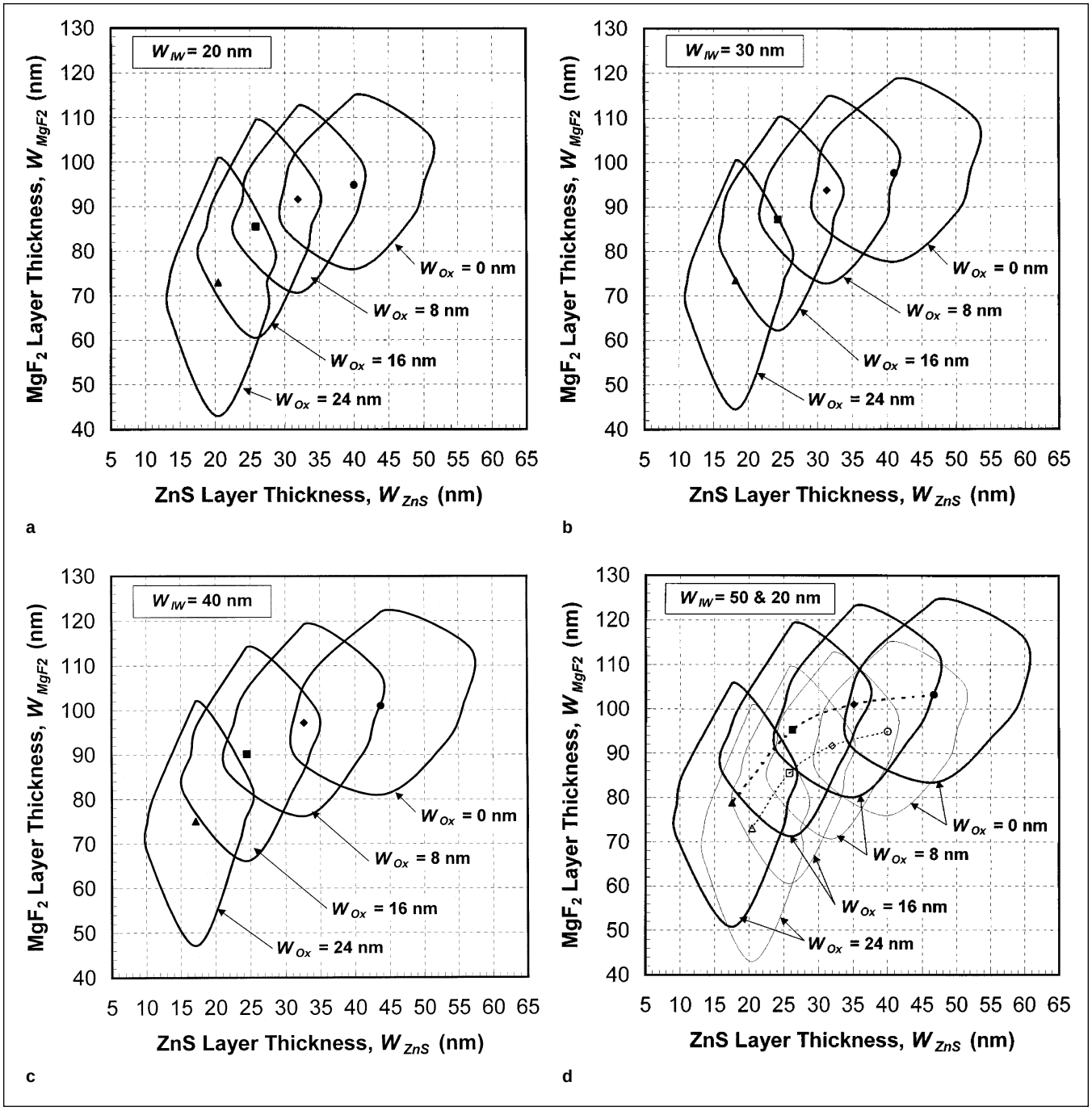

Fig. 4. The quasi-optimum DARC regions and optimum DARCs for several oxidation levels [W_{Ox} = 0 nm (●), 8 nm (◆), 16 nm (■), and 24 nm (▲)]. Aluminum composition is kept constant (x_{Al} = 0.85) as it has been shown that is of little influence. (a) For W_{IW} = 20 nm; (b) For W_{IW} = 30 nm; (c) For W_{IW} = 40 nm; (d) For W_{IW} = 50 nm (thick solid line) and W_{IW} = 20 nm (thin solid line). The optimum DARCs for W_{IW} = 50 nm are linked with a thick dashed line and those for W_{IW} = 20 nm with a thin dashed line.

ZnS and AlGaAs oxide play in the DARC as intermediate refractive index materials. Thus the ZnS layer optimum thickness is reduced more or less in an amount equal to the oxide thickness beneath (rule of thumb proposed in Part I).[1] Moreover oxide growing implies window thinning since part of the AlGaAs window is dissolved to form the oxide. Besides optimum DARC relocation, a general stretching of the quasi-optimum area shape (horizontal shrinkage and vertical enlargement) is observed with increasing oxide layer thickness. This stretching is related again to the window thinning which results from oxide formation. As the oxide grows, a high index layer (namely the AlGaAs window) is substituted by an intermediate index one (the AlGaAs oxide) restricting the critical thickness of the intermediate index layer of the DARC (ZnS) while relaxing the requirements for the low index one (MgF_2).

No influence is observed in quasi-optimum region shape with window thickness. The same trend de-

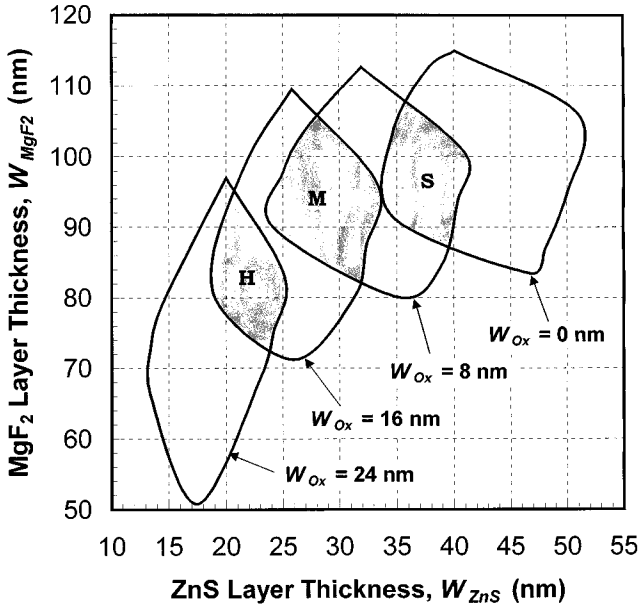

Fig. 5. The quasi-optimum DARC areas for any window layer thickness between 20 nm and 50 nm and any aluminum content from 0.7 to 0.9 for several oxidation levels.

scribed in the previous section for the non-oxide case—the thicker the window, the larger the resulting quasi-optimum area—is still present for all oxidation stages considered. The role of window size on the optimum DARC location can be inferred from Fig. 4d, where the quasi-optimum regions for W_{IW} = 50 nm (thick solid line) have been plotted together with the quasi-optimum regions for W_{IW} = 20 nm (thin solid lines) for comparison. The curve formed by linking the optimum DARCs for W_{IW} =50 nm (thick dashed line) seems to be parallel to its analogous one formed with optimum DARCs for W_{IW} = 20 nm (thin dashed line) but with a larger curvature radius. As in the non-oxide case, thinner windows require smaller W_{MgF2} values to form the optimum DARC. The tendency for W_{ZnS} is not so clear due to the oxide interference (remember the fact that ZnS and AlGaAs oxide have the same role in the ARC). Therefore the optimum W_{ZnS} also decreases together with window thickness for moderate oxidation levels until that trend is eventually stopped or even slightly reversed for thick oxide thickness.

As in the former section, it is interesting to analyze the regions resulting from the intersection of the quasi-optimum DARC regions in Fig. 4a to d which, in turn, produces Fig. 5. Each area plotted in Fig. 5 represents a quasi-optimum DARC region for a certain oxidation level (W_{Ox} = 0, 8, 16, 24 nm) valid for any thickness between 20 nm and 50 nm ($20 < W_{IW} < 50$ nm) and all aluminum contents between 0.7 and 0.9 ($0.7 < x_{Al} < 0.9$). These newly defined areas—again relatively large in size—more or less resemble the original ones as a certain stretching is observed while increasing oxide layer thickness. The goal now is to cope with uncertainties in oxide layer thickness using this method to achieve nearly optimum DARCs with minimal structure knowledge. For this purpose let us consider again the intersection of these new quasi-optimum regions (shadowed areas in Fig. 5) marked with S, M, and H in Fig. 5. Region S (slight oxidation case) represents the set of DARCs which would warrant almost maximum short circuit current for any window between 20 nm and 50 nm, for any aluminum content between 0.7 and 0.9 and with an oxide layer somewhere in between 0 nm and 8 nm thick. A similar description could be made for region M (medium oxidation, with $8 < W_{Ox} < 16$ nm) and region H (heavy oxidation, where $16 < W_{Ox} < 24$ nm).

Therefore when oxidation is present it is necessary to consider more than one quasi-optimum region and thus a minimal knowledge of our sample will be necessary. In our case the segmentation made of the oxidation levels led to three quasi-optimum regions that cover all possible cases. Hence, to apply the model we will need to be able to determine roughly the thickness of the oxide layer in order to decide what the right quasi-optimum region for the solar cells is. We will introduce several ways of doing this in the following section devoted to the experimental results of this work. On the other hand, if a more accurate knowledge of the window is available, these regions could be reduced to two or just one as in the non-oxide case. For instance, if the window layer thickness is surely known to be 20 nm we could just study the intersections in Fig. 4a which eventually give two quasi-optimum regions or even a single one if the possibility of oxides thicker than 16 nm is rejected due to experimental evidence. Nevertheless, it is obvious that when we load our calculations with more and more degrees of freedom (i.e., wide W_{IW} interval as well as wide x_{Al} interval together with broad oxidation intervals) the resulting quasi-optimum regions become considerably smaller, which may conflict with our own manufacturing capability in the method for depositing a DARC.

In fact, up to now the considerations made assume uncertainties in window layer parameters but nothing has been told about the layers forming the DARC. Of course the quasi-optimum region approach is perfectly valid if uncertainties exist in W_{MgF2} and W_{ZnS}, which is indeed a rather common situation. For instance, thermally evaporated DARCs will show a dispersion in layer thickness due to the cosine-law [9-10] distribution of the radiated material. Thus, if uniformity is not granted by planetary rotation or by other means, points in the target plane normal to the radiating boat will receive a different amount of material than those that see the boat with a certain angle. If several boats are present (as in our case, where we have a different boat for each species in the DARC) the tolerances are even bigger. In such situations the quasi-optimum approach provides an ideal frame to design ARCs as a broad interval of both W_{MgF2} and W_{ZnS} is available to achieve optimum performance. We just have to be sure that the technological tolerance associated with the deposition process lies within the boundaries of the calculated quasi-optimum region of interest.

Table II. A Summary of the Experiments Carried Out*

	Window Parameters			Applied ARC			Results		
Exp. #	W_{IW} (nm)	x_{Al} (%)	W_{Ox} (nm)	Q.O. Region	W_{ZnS} (nm)	W_{MgF2} (nm)	Comments	ΔJ_{SC}	J_{SC} [15] (mA/cm²)
1	15	81	≈7	S	36	96	Centered in S	35 %	25.0
2	15	81	≈0	N.O.	44	97	Centered in N.O.	35 %	25.3
					31	98	Centered in M	32%	25.7
3	20	85	≈12	M	38	99	Centered in S	30%	25.2
					45	99	Centered in N.O.	25%	24.2
					31	93	Centered in M	26 %	24.3
4	22	81	≈7	S	38	97	Centered in S	33 %	25.7
					44	97	Centered in N.O.	32 %	25.2
					35	103	Border S-N.O.	27 %	25.6
5	30	85	≈0	N.O.	45	100	Centered in N.O.	30 %	26.0
					50	100	Right Border N.O.	26 %	25.2
					37	97	Centered in S	32 %	25.9
6	50	87	≈8	S-M	41	102	Border S-N.O.	27 %	24.9
					55	109	Right Border N.O.	22 %	24.0

*Horizontal lines separate different cell batches (i.e. different processing and/or different structure). The quasi-optimum regions (Q.O.) are named as in Fig. 6, i.e. N.O. for no-oxidation, S for slight oxidation, M for medium oxidation and H for heavy oxidation.

EXPERIMENTAL RESULTS

Experiment Setup

To apply the proposed model a certain knowledge of the oxidation level of the window is required. Many refined methods are available for determining the surface parameters of the sample including a whole variety of sophisticated surface analysis/scanning techniques (Auger, SIMS, RBS, etc.). However we have found the analysis and fitting of reflectance measurements, namely Optical Reflectance Spectroscopy (ORS),[1,11–14] extremely accurate, reliable and simple.[13]

In addition, this knowledge could be obtained from a very simple experiment. It would be enough to take three batches of identical cells (with the same structure and processing) and to cover them with three DARCs from all of the quasi-optimum regions: S, M, and H. The batch obtaining the maximum increase in short circuit current would be the one with the right DARC and thus would show us the quasi-optimum region to work with. The choice between the different characterization procedures is of course a trade-off between accuracy, simplicity and reliability.

In order to validate experimentally the approach for the DARC design proposed here, a wide variety of MgF_2/ZnS DARCs were deposited by vacuum thermal evaporation with standard conditions as that in Part I.[1] The performance of solar cells—mainly short circuit current and spectral response—was measured both before and after the DARC deposition to evaluate the changes in cell parameters. All cells used in this experiment were typical p on n heteroface AlGaAs/GaAs concentrator solar cells manufactured by MOCVD (Fig. 1a of Part I).[1]

Results and Discussion

The experimental data herein presented are the results of the cells produced in our lab over a period of several months (around 2000 devices). During that period the model was applied to the available samples. However no special designs were made to test our new approach. For this reason collected experimental data provides a good basis to validate this model experimentally although it does not include evidence for all cases necessary to fully determine the perfect matching between theory and practice. Table II includes a summary of the processed samples.

Every time a new set of cells was processed its window parameters were checked by means of ORS. This led to an estimate of the window parameters (columns 2 to 4 of Table II) which helped us in the choice of the quasi-optimum region to use (column 5). Columns 6, 7, and 8 in Table II summarize the characteristics of the DARC actually applied. Together with the optimum, several different DARCs were also tested in order to evaluate the accuracy and reliability of the predictions of the model. For instance, in some cases DARCs coming from the quasi-optimum region for the non-oxide case (Fig. 3) were deposited to evaluate the cost of ignoring the oxide layer. In other cases, representative DARC coatings from different regions or on the edge of a region were used. The column number 8 in Table II indicates the approximate location of a given DARC. Finally, the performance of the coatings is analyzed in terms of the net increment in short circuit current (ΔJ_{SC}) that they produce and its absolute value[15] (J_{SC}) in columns 9 and 10 of Table II.

The first two experiments in Table II show very good agreement between theory and practice. In the first case a thin oxide layer was detected and thus region S was used for DARC deposition. Virtually the same results were achieved in experiment 2 where no oxide was detected and a non-oxide DARC was deposited. This fact is in agreement with the assessment

made in a previous section that variations of the DARC within the quasi-optimum region will not cause a significant variation in the final short circuit current value.

In experiment 3, an oxide layer of around 12 nm (region M) was detected by ORS, while an oxide layer of some 7 nm (region S) was found in experiment 4. In both experiments some cells were coated with a typical DARC from region M, some other cells were covered with a DARC from region S and finally a DARC from the non-oxide case was also tested. The best increment in short circuit current was obtained in both cases with the DARC belonging to the quasi-optimum region (M in experiment 3 and S in 4). This is again in excellent agreement with the behavior predicted. The smaller values for the ΔJ_{SC} achieved in these experiments could be due to the oxide acting as a native ARC, improving the reflectance of the bare cells.[1] The high optimum values obtained for J_{SC} support the former hypothesis. The evolution of DARC performance in regions adjacent to the quasi-optimum region deserves an extra comment. In experiment 3 the DARC from region M is better than that from region S, and the former is better than that from the N.O. region. Similarly, in experiment 4 we have that region S is better than region N.O. which is itself better than region M. This evolution seems to indicate that around the optimum value, the decrease in performance has a higher gradient when assuming thicker oxides than when underestimating oxide thickness. In other words, when in doubt it seems better to assume lower thickness for the oxide layer in order to get better short circuit current increments.

Let us now look at both the last two experiments in Table II (5 and 6), involving thick windows. In experiment 5 ORS results showed that there was no oxide layer present. This circumstance was exploited to verify the accuracy of the study of the non-oxidation case. Three DARCs were chosen within the no-oxide quasi-optimum region, one more or less centered and the other two with extreme W_{ZnS} values (i.e., one in the boundary of the region S and the other on the right edge of the N.O. region). Regarding experiment 6, three DARCs were considered: a centered S-region DARC, a non-oxide DARC and an intermediate DARC on the edge of S-region. This time a clear improvement in short circuit current was obtained with the DARC of region S compared to the others.

These two experiments again follow very well the qualitative evolution predicted by the theory. The best ΔJ_{SC} is obtained with DARCs in the center of the appropriate quasi-optimum region deduced from ORS measurements. In addition, the absolute short circuit current values obtained for such centered DARCs are among the best values reported in literature ($J_{SC} \approx 26$ mA/cm^2)[15] for the shadowing factor herein considered ($F_S = 7.2\%$). However extreme DARCs still belonging to the quasi-optimum region produced a larger than expected drop in ΔJ_{SC}(2–3 points absolute). This is in clear disagreement with our design requirement forcing the DARCs that belong to the same quasi-optimum region to grant virtually the same performance. This fact suggests that for thick windows the sensitivity of the DARC is higher than predicted in our model for unknown reasons.

A possible cause for such behavior could be related to the poor quality of the layers making up the DARC (voids, little homogeneity, etc.) in some particular deposition process. The role of voids has been studied by other authors for silicon solar cells[16] but is not considered in our model and thus will be the subject of a future work. Another potential source of disagreement between the model and the experimental evidence encountered could come from the fact that aluminum contents in experiment 6 were close to the upper limit ($x_{Al} = 0.9$) for the interval of application of the model used to describe the oxide refractive index.[1]

The cells studied in the experimental phase that showed some degree of oxidation belong to quasi-optimum regions S and M. Experimental evidence of oxide layers belonging to region H (and even thicker) has been reported in other works.[14] The reason for not finding them in our study is probably because the maximum aluminum content of our samples was 87% instead of 91% as in Ref. 14.

As a general conclusion we could say that the limited experimental data available has shown good agreement with the model developed. In particular, very good results—both qualitative and quantitative—have been obtained for thin windows with any oxidation level. Thick windows seem to be more sensitive than predicted, but there is not enough reliable data to assess this accurately. More experimentation is needed.

SUMMARY AND CONCLUSIONS

A modified model for MgF_2/ZnS double antireflection coating design for AlGaAs/GaAs heteroface solar cells has been presented, extensively analyzed and experimentally tested. The main contribution of this model is that it takes uncertainties in the parameters involved in ARC optimization into account. This approach is based on the concept of quasi-optimum DARC regions—instead of classical optimum DARCs—defined as the set of W_{MgF2}-W_{ZnS} pairs that provide an antireflection performance virtually equal to that of the optimum for a certain variable range of optically relevant parameters (x_{Al}, W_{IW}, W_{Ox}). Being able to choose in an interval of quasi-optimum values that provide the best antireflecting results helps us to deal with either dispersion in cell parameters or tolerances in DARC deposition.

When no oxidation is present (the classic case) the calculated quasi-optimum region—valid for all windows between 20 nm and 50 nm thick and all aluminum contents from 0.7 to 0.9—roughly extends from $35 < W_{ZnS} < 50$ nm to $90 < W_{MgF2} < 110$ nm (the exact shape is shown in Fig. 3). The region includes all previously published optimum data (to our knowledge) as particular cases.

When oxidation is present, a minimal estimate of the oxide thickness is needed to apply the model. For

this task a simple experiment or a more sophisticated technique based on reflectance measurements has been recommended to determine both oxide and window characteristics. Once the oxide is catalogued in one of the three oxidation stages considered, a tailored quasi-optimum region can be used for DARC design (the exact shape is shown in Fig. 5). These are as follows:

- Region S (slight oxidation, 0 nm $< W_{Ox} <$ 8 nm) which roughly extends from $35 < W_{ZnS} < 40$ nm to $90 < W_{MgF2} < 102$ nm.
- Region M (medium oxidation, $8\,nm < W_{Ox} < 16\,nm$) which roughly extends from $26 < W_{ZnS} < 31$ nm to $89 < W_{MgF2} < 100$ nm.
- Region H (heavy oxidation, $16\,nm < W_{Ox} < 24\,nm$) which roughly extends from $20 < W_{ZnS} < 25$ nm to $77 < W_{MgF2} < 87$ nm.

The model presented has yielded very good results for both oxidized and non-oxidized samples, as demonstrated by the systematically high short circuit current values (J_{SC} = 25–26 mA/cm^2 at one sun AM1.5D spectrum for F_S = 7.2%) obtained for a wide variety of situations. These values are among the best values reported in existing literature (to our knowledge) and have been confirmed externally. Particularly, for thick windows, the qualitative evolution shown was as predicted by the model but quantitative variations in J_{SC} were larger than expected for DARC values placed on the edge of the quasi-optimum regions. On the other hand, thin windows have shown excellent agreement—both qualitative and quantitative—between experiments and theoretical predictions.

ACKNOWLEDGEMENTS

This work has been financed through the JOULE-THERMIE Program of the European Union under contract JOR3-CT97-0123, through the National Renewable Energies Program of the Spanish Bureau for Science and Technology (CICYT) under contract TIC96-0725-C02-01 and through the Environmental Technologies Program of the Autonomous Government of Madrid.

REFERENCES

1. I. Rey-Stolle and C. Algora, *J. Electron. Mater.* 29, 984 (2000).
2. C. Algora and M. Felices, *IEEE Trans. Electron Dev.* 44, 1499 (1997).
3. M.E. Nell et al., *Proc. 10th European Photovoltaic Solar Energy Conf.* (Dordrecht, The Netherlands: Kluwer Academic Publishers, 1991), p. 545.
4. N.D. Arora and J.R. Hauser, *J. Appl. Phys.* 53, 8839 (1982).
5. A. Yoshikawa and H. Kasai, *J. Appl. Phys.* 52, 4345 (1981).
6. G, Habermann, A. Bett, F. Lutz, C. Schetter, O.V. Sulima, and W. Wetlling, *Proc. 11th European Photovoltaic Solar Energy Conf.* (Chur, Switzerland: Harwood Academic Publishers, 1993), p. 217.
7. T.A. Gessert and T.J. Coutts, *J. Vac. Sci. Technol. A* 10, page (1992).
8. D.J. Friedman, S.R. Kurtz, K.A. Bertness, A.E. Kibbler, C. Kramer, and J.M. Olson, *Proc. First World Conf. Photovoltaic Energy Conversion* (Publisher's City: Publisher's Name, 1994), p. 1829.
9. O.S. Heavens, *Optical Properties of Thin Solid Films* (New York: Dover Publications Inc., 1991).
10. S.K. Gandhi, *VLSI Fabrication Principles for Si and GaAs*, 2nd ed. (New York: John Wiley and Sons, 1994).
11. L.E. Tarof, *Appl. Optics* 27, 4798 (1988).
12. L.E. Tarof, C.J. Miner, and A.J. Springthorpe, *J. Electron. Mater.* 18, 361 (1989).
13. C. Algora, *J. Electron. Mater.* 29, 436 (2000).
14. M.M. Sanfacon and S.T. Tobin, *IEEE Trans. Electron Dev.* 37, 450 (1990).
15. Measurements for the best cells in these experiments have been externally confirmed by the National Renewable Energy Laboratory in Golden, Colorado.
16. H. Nagel, A.G. Aberle, and R. Hezel, *Prog. Photovolt: Res. Appl.* 7, 245 (1999).